Eur. Phys. J. D **35**, 199–205 (2005)
DOI: 10.1140/epjd/e2005-00089-5

THE EUROPEAN PHYSICAL JOURNAL D

Electron attachment to strongly polar clusters

Formamide molecule and clusters

M. Seydou[1,2], A. Modelli[3], B. Lucas[1], K. Konate[2], C. Desfrançois[1], and J.P. Schermann[1,a]

[1] Laboratoire de Physique des Lasers, UMR7538, Institut Galilée, Université Paris 13, 93405 Villetaneuse, France
[2] DER de Physique, Faculté des Sciences et techniques, Bamako, BPE3206, Mali
[3] Dipartimento di Chimica, "G. Ciamician", Universita di Bologna, via Selmi 2, 40126 Bologna, Italy
and
Centro Interdipartimentale di Ricerca in Scienze Ambientali (CIRSA), via S. Alberto163, 48100 Ravenna, Italy

Received 11 March 2005
Published online 14 June 2005 –

Abstract. Electron localization is studied in formamide cluster anions. The isolated formamide molecule has a large dipole moment and its clusters can give birth to multipole-bound anions as well as valence anions. The vertical valence electron affinity of the isolated molecule is determined by electron transmission spectroscopy. The anion formation process is studied as a function of cluster size with Rydberg electron transfer spectroscopy. DFT calculations of the neutral and negatively-charged cluster structures show that the anion excess electron localizes on a single molecule. The adiabatic valence electron affinity of isolated formamide is deduced from the observation of the cluster size threshold for valence attachment.

PACS. 34.80.Gs Molecular excitation and ionization by electron impact – 36.40.Mr Spectroscopy and geometrical structure of clusters – 87.15.By Structure and bonding

1 Introduction

Different low-energy electron attachment processes compete in polar molecular systems. Excess electrons can enter molecular orbitals in conventional (valence) anions or remain located nearly totally outside the molecular frame in multipole-bound anions. Multipole-bound anions can only be created if the dipole and/or quadrupole moments of the parent systems exceed critical values [1,2]. Clusters of molecules with individual dipole moments below the critical value ca. 2.5 D can also bind excess electrons either internally as in solvated electrons or in diffuse orbitals as surface states or multipole-bound states [3–5]. When the valence electron affinity of the constituting polar molecule is negative, transient valence anion formation appears as a resonance in the free-electron scattering cross-section of the neutral monomer [6]. When polar molecules are embedded in a cluster, the total multipole (dipole and/or quadrupole) moments of the most stable configurations can exceed or be lower than the critical values [7] and excess electrons can be bound or not, then leading to magic numbers in the anion mass-spectra [8,9]. When the cluster size further increases, solvation effects become more and more important and valence electron binding enters into competition with electron multipole binding. Above a threshold size value N_{th}, the cluster valence electron affinity becomes positive and a smooth anion mass distribution is observed.

In the most widely studied case of anion water clusters, the mass-spectra exhibit magic numbers ($N = 2, 6, 7$) and become smooth above $N_{th} = 10$ [10–12]. In ammonia clusters, there are no magic numbers and a smooth mass-spectrum is observed for cluster sizes above $N_{th} = 33$ [10,12]. Both water and ammonia have a dipole moment much smaller than the critical value for electron binding. The theoretical interpretation of the observed mass-spectra is then very difficult and the structure of water anions is still the subject of elaborated experimental [5,9] and theoretical studies [2,8].

In the present work, our attention is focused on valence electron attachment to the isolated formamide molecule which possesses a dipole moment of 3.72 D, much larger than the critical value, and to its homogeneous clusters. In gas-phase collisions, the isolated formamide molecule can temporarily attach a free electron of appropriate energy and angular momentum into a vacant MO, the process being referred to as a shape resonance [13]. Electron transmission spectroscopy (ETS) [14] is one of the most suitable means for detecting the formation of such short-lived anions. Because electron attachment is rapid with respect to nuclear motion, the temporary anion is formed in the equilibrium geometry of the neutral molecule. The impact electron energy at which electron attachment occurs is properly denoted as vertical attachment energy (VAE)

[a] e-mail: scherman@galilee.univ-paris13.fr

and is the negative of the vertical electron affinity. The ETS spectrum of isolated formamide is here reported for the first time.

We also here consider electron binding to formamide clusters. The electron source is then a laser-excited Rydberg atom source [12,15]. We have already shown that the magic island ($N = 1, 2$ and 3), which appears in the formamide anion mass-spectrum observed in collisions between Rydberg atoms and neutral formamide clusters, can be interpreted in terms of creation of multipole-bound anions [16]. This interpretation has been confirmed by means of infrared spectroscopy which provides information about the geometrical structures of the neutral precursor of the formed anion [17].

Since formamide is an important model compound for hydrogen bonding and peptide linkage, the structures of the neutral parent clusters have been widely theoretically studied but, to our knowledge, the only studied ionized formamide clusters are either the protonated clusters up to $N = 3$ [18] or the multipole-bound anions up to $N = 3$ [16]. The experimental results of a rather similar study of electron attachment to N-monosubstituted amide clusters up to large values ($N = 23$) have been published [19] and will be compared to the present results. From the experimental observation of the size threshold for valence electron attachment and calculations of binding energies of both neutral and anion clusters, we here deduce the valence adiabatic electron affinity of formamide which we compare to theoretical predictions.

2 Experimental procedure

2.1 Electron transmission spectrum

The electron transmission apparatus presently used is in the format devised by Sanche and Schulz [14] and has been previously described [20]. To enhance the visibility of the sharp resonance structures, the impact energy of the electron beam is modulated with a small ac voltage, and the derivative of the electron current transmitted through the gas sample is measured directly by a synchronous lock-in amplifier. Each resonance is characterized by a minimum and a maximum in the derivative signal. The energy of the midpoint between these features is assigned to the most probable VAE. The present spectrum was obtained by using the apparatus in the "high-rejection" mode [21] and is, therefore, related to the nearly total scattering cross-section. The electron beam resolution was about 50 meV (fwhm). The energy scale was calibrated with reference to the $(1s^1 2s^2)^2$S anion state of He which energy is 19.37 eV at its minimum in the derivatised signal. The estimated accuracy is ±0.05 eV.

The results of our ET measurements in H_2NCHO are shown in Figure 1, where the derivative of the transmitted current is plotted as a function of the electron impact energy over the range from 0.5 to 6 eV. The ET spectrum displays a single distinct resonance, located at 2.05 eV (fwhm = 0.82 eV). Such an intense feature is expected to be associated with electron capture into the empty π^*_{CO} MO (Fig. 2a). A corresponding resonance has been observed in the ET spectra of formaldehyde [22] (VAE = 0.86 eV), acetone [23] (VAE = 1.31 eV) and cyclic monoketones [23,24] (VAE = 1.00, 1.15 and 1.30 eV for the four-, five- and six-membered cycles, respectively). The destabilisation (about 1 eV) caused by the amino substituent on the π^*_{CO} anion state is in line with previous ET data, and has been ascribed to charge-transfer interaction with the adjacent nitrogen lone pair [23].

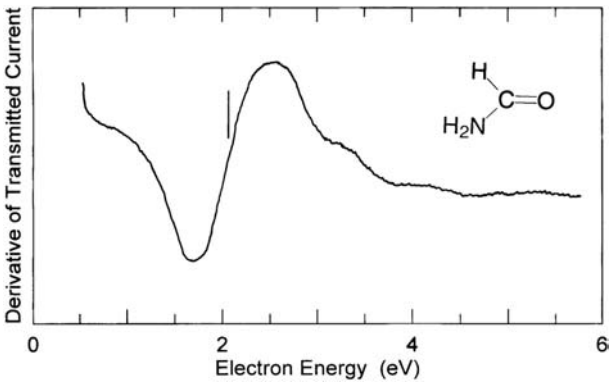

Fig. 1. Derivative of the electron current transmitted through formamide vapour, as a function of the electron energy. The vertical line locates the VAE.

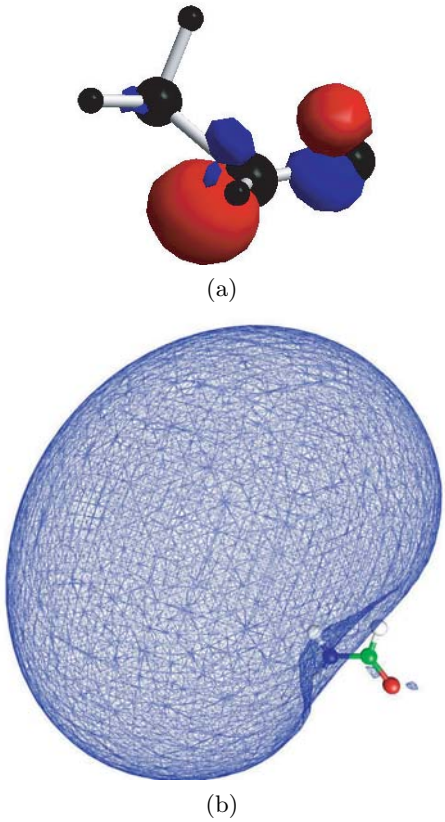

Fig. 2. Excess electron orbital: (a) in the formamide monomer valence anion; (b) in the formamide monomer dipole-bound anion.

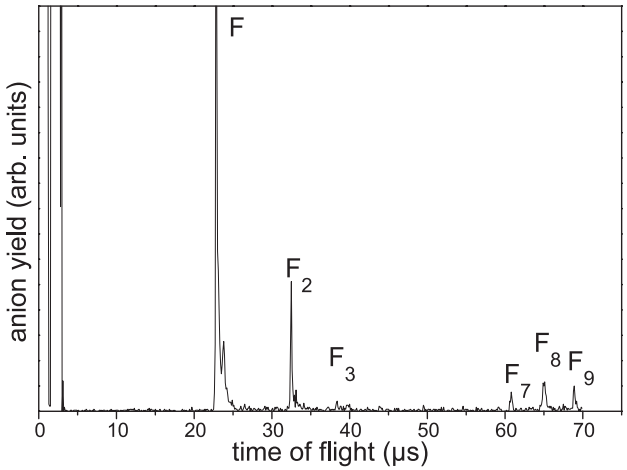

Fig. 3. Mass spectrum of formamide anions created in charge-transfer collisions between Rydberg ($15f$) xenon atoms and neutral formamide clusters. For F, F_2 and F_3, the anion yields strongly depend upon the n principal quantum number n of the Rydberg atoms [16]. The quantum number $n = 15$ optimises the yield of quadrupole-bound dimer anions while the trimer anion yield reaches an optimum for $n = 13$ and thus appear here as negligible. On the contrary, the anion yields for the larger cluster anions ($N > 6$) vary smoothly with n and are thus characteristic of valence anion formation [47].

2.2 Rydberg electron transfer

Electron attachment to neutral clusters has been studied with a crossed-beam set-up which has been previously described. Cold neutral clusters are produced by expanding few tens of mbars of formamide vapour, obtained in an oven at 80 °C, in 3 bar of helium through a heated pulsed valve with a 0.15 mm hole maintained at 110 °C. This supersonic molecular beam, skimmed by a heated cone, crosses a beam of laser-excited Xe Rydberg atoms with principal quantum number varying between 9 and 25. Following electron transfer from the Rydberg Xe atoms to the molecular clusters, anions are produced and mass-analysed in a Wiley-McLaren tube with time-of-flight in between 20 and 70 μs. The signatures of the electron attachment processes leading to anion production are the Rydberg n-dependences of the formamide anion creation rates. In reference [16], it is shown that formation of multipole-bound anions corresponds to sharply peaked n-dependences and are observed for the formamide monomer, dimer and trimer. Formation of valence anions corresponds to smoothly varying n-dependences that are observed for production of all cluster formamide anions above a sharp threshold value of $N = 7$ (Fig. 3). Similar threshold values of 6 or 7 have been observed in a series of N-monosubstituted amide clusters $(\mathrm{XCO-NHY})_N^-$; X, Y = H, $\mathrm{CH_3}$, $\mathrm{C_2H_5}$ [19].

The striking difference between the observed Rydberg n-dependences in multipole electron binding and valence electron binding comes from the difference between the electron-molecule interaction ranges. In multipole electron binding, the exchanged electron switches from a very diffuse atomic orbital to a very diffuse molecular orbital (Fig. 2b). Electron transfer only takes place when the classical frequencies of this electron are nearly equal in both orbitals. In valence electron binding, the electron-molecule interaction has a very short range as compared to the atomic ionic core Xe^+ electron interaction. The situation is analogous to that encountered in the Fermi model for Rydberg electron collisions [25] and the Rydberg electron behaves as a nearly-free electron. The variation of the electron transfer rate becomes a smooth function of the Rydberg principal quantum number [15,25].

2.3 Computational details

Calculations concerning the valence electron attachment to the monomer were performed with the Gaussian 98 set of programs [26]. Geometry optimisations and the virtual orbital energies (VOEs) of isolated neutral formamide were evaluated using Hartree-Fock (HF), second order many-body perturbation theory (MP2) and density functional theory B3LYP calculations, with the standard 6-31G and 6-31G* basis sets. The VAE of formamide was calculated as the difference of the total energy of the neutral and the lowest anion state, both in the optimised geometry of the neutral state, using the B3LYP hybrid functional with the 6-31G* and 6-31+G* basis sets.

For clusters, we used the simple basis 6-31G* since we are here interested only in valence electron binding. We do not add the very diffuse orbitals that would be required for taking into account dipole electron binding [2]. Since we calculate energy differences between neutral and anion structures of the same species, we do not correct for basis set superposition errors (BSSE). In order to test the accuracy of the DFT calculations, we have compared the binding energies of both neutral and anions predicted by DFT and MP2 with the 6-31G* basis set. For the neutrals, DFT calculations provide very similar geometries and binding energies which are only 0.15 eV larger than those of MP2, but there is a larger uncertainty of ± 0.3 eV for the anions.

3 Results and discussion

One of our aims is the determination of the valence vertical and adiabatic electron affinity of the isolated formamide molecule. Free-electron attachment takes place vertically and the electron transmission experiment provides us the vertical value which is here negative. In absence of an environment, autodetachment takes place extremely rapidly and no formamide anion is observable with free electrons. Our hypothesis is that, due to the very large dipole moment of formamide or the very large quadrupole moment of its dimer that are both larger than the critical values for multipole electron binding [27], the excess electron first localizes on a monomer or a cluster subsystem in a diffuse orbital and then enters a valence orbital if this becomes energetically more favourable. We will thus a priori exclude the possibility of collective binding as in solvated

electron models. If the nascent formamide anion is embedded in a molecular environment, energy transfers tend to stabilise this anion by spreading its internal energy into the intermolecular modes. If the anion is totally relaxed, the valence electron affinity which must be considered is the adiabatic electron affinity. Adiabatic valence electron affinities are difficult to obtain either experimentally or theoretically when they are negative. In fact, they may not even exist if the lifetimes of the temporary anions do not allow vibrational relaxation to take place before autodetachment.

3.1 Vertical valence electron affinity of isolated formamide

The ET spectrum of formamide shows that the first vertical electron affinity (EA_v), associated with temporary electron attachment to the empty π^*_{CO} MO, is sizeably negative (−2.05 eV). This result is in line with previous observations [23,24,28] of the large destabilising effect (about 1 eV) caused on the π^*_{CO} anion state by mixing with an adjacent oxygen or nitrogen lone pair.

A theoretical approach adequate for describing the energetics of the unstable anion states observed in ETS involves difficulties not encountered for neutral or cation states. The first VAE can in principle be obtained as the energy difference between the lowest-lying anion and the neutral state (both with the optimised geometry of the neutral species). A proper description of spatially diffuse species requires a basis set with diffuse functions. However, as the basis set is expanded, an SCF calculation ultimately describes a neutral molecule and an unbound electron in as much of the continuum as the basis set can emulate. Stabilisation procedures are then needed to distinguish the virtual orbitals that give rise to temporary anion states from those low-energy solutions having no physical significance with regard to the resonance process [29–33]. It has also been shown [33] that this effect increases with increasing instability of the anion state. Here, in formamide, increasing the basis set also leads to the prediction of a dipole-bound state [17].

We have here evaluated the first VAE of formamide as the anion/neutral state energy difference at the B3LYP level with the 6-31G* and the 6-31+G* basis sets. The 6-31G* basis set describes both the LUMO of the neutral state and the SOMO of the lowest-lying anion state as a valence π^*_{CO} MO, but the predicted VAE (3.796 eV) is by far too large. The 6-31+G* basis set (the minimal basis set which includes diffuse functions) yields a VAE (1.180 eV) sizeably smaller than the experimental value. In addition, both the LUMO and SOMO are described as rather spatially diffuse σ^* MOs mainly localized on the HCN skeleton, in line with previous results on benzene and ethyne [32].

The Koopmans' theorem (KT) approximation neglects correlation and relaxation effects, which tend to cancel out when ionization energies, but not electron affinities, are evaluated. Consistently, the calculated empty orbital energies overestimate the measured VAE by several eV. However, Chen and Gallup [29] found a good linear correlation between the virtual orbital energies (VOEs) supplied by simple HF/6-31G calculations and the corresponding experimental VAEs. In a more extended study of the use of KT calculations for the evaluation of VAEs, Staley and Strnad [30] demonstrated the occurrence of good linear correlations between the $\pi^*_{C=C}$ VAEs measured in a large number of alkenes and benzenoid hydrocarbons and the corresponding VOEs obtained with HF or MP2 calculations, using basis sets which do not include diffuse functions. More recently an analogous linear correlation has been found between π^* VAEs and the corresponding VOEs supplied by B3LYP/6-31G* calculations [32]. In contrast, inclusion of diffuse functions led to a breakdown in the correlation [30,34].

Table 1. Virtual orbital energies (VOEs) of formamide, scaled VOEs (in parentheses — see text), and experimental VAE. All values in eV.

orbital	B3LYP/6-31G*	HF/6-31G	MP2/6-31G*	expt. VAE
σ^*_{HCN}	2.951	6.862	6.903	
σ^*_{NH}	1.961	5.912	5.894	
π^*_{CO}	0.809 (1.86)	5.079 (1.84)	5.349 (2.04)	2.05

Table 1 reports the lowest-lying VOEs of neutral state formamide supplied by B3LYP/6-31G*, HF/6-31G and MP2/6-31G* calculations. In all cases, the LUMO is predicted to be the π^*_{CO} MO. The closest agreement is found with the MP2/6-31G* calculations which nicely reproduce also the π^*_{CO} VAE of unsubstituted formaldehyde [24].

In a recent study of dissociative electron attachment to formic acid [35], the $HCOO^-$ current peaking at 1.25 eV (as well as the resonance displayed at 1.8 eV in the ET spectrum) was associated with the first 3 or 4 virtual orbitals, remarkably diffuse and with no particular valence character. This assignment, based on theoretical results obtained with the aug-cc-pVTZ basis set (which includes even more diffuse functions than the 6-311+G* basis set), disagrees with all previous assignments of the ET spectra of carbonyl [32] derivatives and does not provide a mechanism by which such diffuse states could lead to intense signals in the ET and DEA spectra. The present results confirm the expectation of the valence π^*_{CO} character of the lowest-lying resonance of formamide and once again point out that the choice of a basis set that gives a satisfactory description of the energy and nature of the resonance processes is a delicate task. In particular, when diffuse functions (representing the neutral molecule with the electron in the continuum) are used much care is needed to distinguish the solutions associated with anion state formation from those which have no significance with regard to the resonant electron capture process.

3.2 Influence of solvation upon valence electron affinities

Let us consider the adiabatic valence electron affinity (AEA) of the formamide clusters (Fig. 3). The AEA is

defined as the energy difference between the electronic energy of the neutral formamide cluster with full geometry optimisation and the electronic energy of the fully optimised formamide cluster anion at its equilibrium geometry including zero-point energy corrections (ZPE)

$$AEA(F_N) = AEA(F) + E(\text{optimised neutral cluster } F_N) + ZPE(F_N) - E(\text{optimised cluster anion } F_N^-) - ZPE(F_N^-). \quad (1)$$

The energies $E(F_N)$ and $E(F_N^-)$ are the formation energies of F_N and F_N^- relative to the dissociated constituents N times F and $(N-1)$ times F plus F^-, respectively. In a F_N^- formamide cluster anion, the excess electron can be localized on a single F molecule, on a F_P sub-cluster $(1 \leq P \leq N)$ [36] or can be collectively bound by the N molecules. Due to the presence of large attractive charge-dipole interactions in the anions, the stabilisation energy $E_{sol}^{anion}(N)$ of a F_P^- anion solvated by Q neutral molecules, with $P+Q=N$, is larger than the stabilisation energy $E_{sol}^{neutral}(N)$ of the corresponding F_P neutral by the Q neutral molecules. We will further show that the most stable configurations of the formamide anions correspond to the localization of the excess electron on a single molecule $(P=1)$.

The AEA of the neutral clusters F_N becomes less and less negative when N increases. Once N reaches a threshold value N_{th}, the valence AEA becomes positive and the $F_{N \geqslant N_{th}}^-$ cluster anions become experimentally observable.

We obtain a bracketing of the adiabatic value of the electron affinity of formamide by means of the following inequalities [37]

$$E_{sol}^{neutral}(N_{th}) - E_{sol}^{anion}(N_{th}) \leq AEA(F) \leq E_{sol}^{neutral}(N_{th}-1) - E_{sol}^{anion}(N_{th}-1). \quad (2)$$

The experimental value of N_{th} is equal to 7 (Fig. 3) for formamide [16] and we have conducted calculations up to this size. We have here conducted a systematic search of the lowest energy configurations by means of an empirical model following the lines developed by No et al. [38]. The total intermolecular potential energy contains pair interactions and some three-body and higher interactions. A genetic algorithm provides roughly optimised geometries which are further fully optimised by means of quantum calculations.

The neutral formamide cluster configurations have already been experimentally [39–41] and theoretically [42–45] considered by means of different approaches. According to the used experimental methods and the considered gas, liquid or crystal phase, different configurations have been predicted or observed. Among those possible configurations, we have more specifically considered the planar, cyclic and zig-zag structures [44]. We found that the most stable neutral structures are planar as in reference [45]. The even clusters ($N=4$, 6 and 8) are formed by addition of cyclic dimers. They can also be seen as antiparallel chains, forming dipole chains within which each

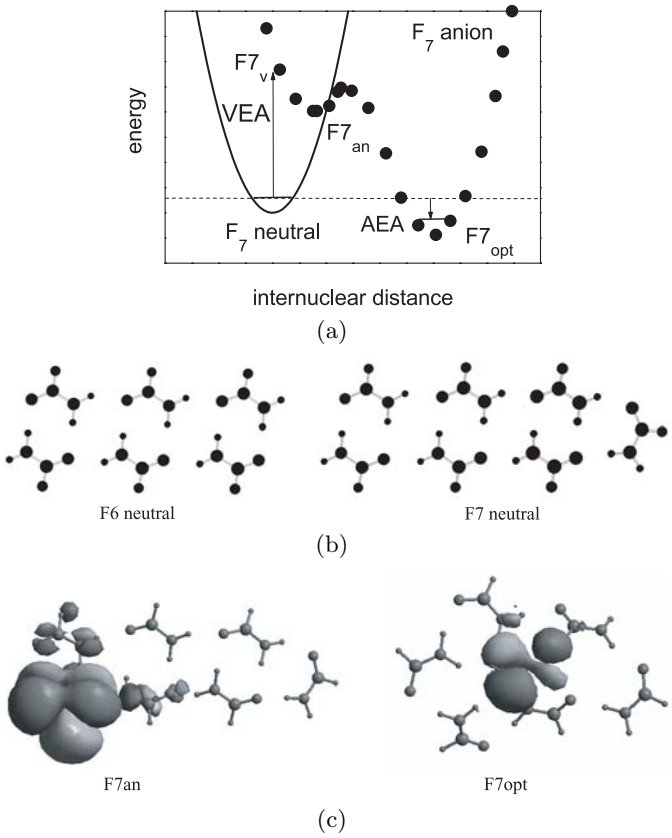

Fig. 4. (a) Schematic potential energy diagram of the neutral (solid line) and negatively-charged formamide heptamer (dotted line). There exist several minima but we here only represent the optimised structure obtained by relaxing the anion created at the neutral geometry ($F7_{an}$) and the most stable structure ($F7_{opt}$) corresponding to the adiabatic electron affinity AEA. The corresponding structures are displayed in (b). (b) Optimised structures of the neutral formamide hexamer and heptamer. (c) Excess electron orbitals in the first optimised anion structure obtained by relaxing the anion created at the neutral geometry ($F7_{an}$) and the most stable anion structure ($F7_{opt}$).

internal formamide is H-bonded to three other molecules. In those nearly linear chains, the dipole-dipole interactions are maximized. For odd clusters ($N=5,7$), these antiparallel chains are capped on one side by a formamide molecule whose dipole moment is oriented perpendicularly to the chains (Fig. 4b) and still prefer dipole-dipole interactions. Those odd planar clusters are less bound than the even planar clusters as already shown in reference [45]. The zig-zag configurations possess much larger dipole moments but much less H-bonds and are thus less favourable, as well as cyclic structures.

Following vertical electron attachment to the most stable (planar) neutral configurations, the corresponding negatively-charged clusters are strongly vibrationally excited and relax towards more stable geometries (FN_{an}, in Fig. 4a). In those excited anion configurations, the excess electrons are localized in valence molecular orbitals on a single or two formamide molecules (Fig. 4c). The most

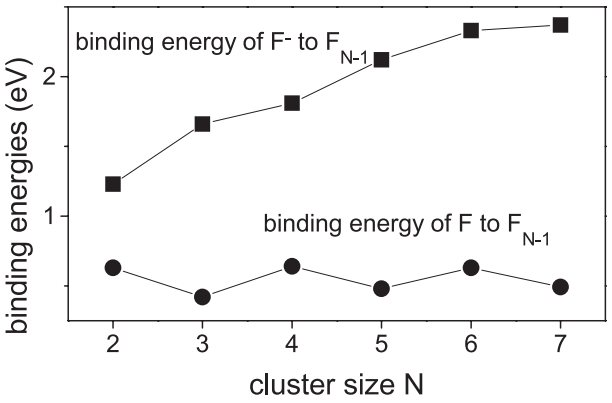

Fig. 5. Stabilisation energies of neutral F_N and negatively-charged F_N^- formamide clusters. The two curves respectively correspond to the calculated stabilisation energies $E[F_N] - E[F + F_{N-1}]$ and $E[F_N^-] - E[F^- + F_{N-1}]$ at the B3LYP/6-31G* level.

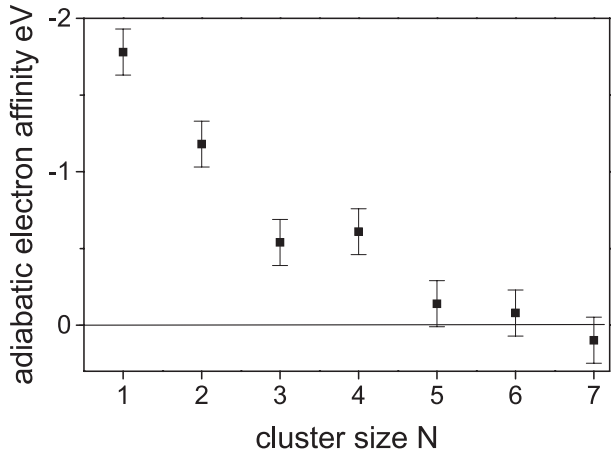

Fig. 6. Calculated adiababatic electron affinity of neutral F_N formamide clusters. The error bars correspond to the uncertainty introduced in the calculation of binding energies in the anion. This uncertainty is due to the use of a rather small basis set (6-31G*) in order to restrict the binding of the anion excess electron into valence orbitals (see text).

stable formamide cluster anion structures correspond to excess electrons localized on a single formamide molecule and are thus solvated anion structures (Fig. 4c). In a F_N^- cluster, the formamide monomer anion is surrounded by a ring of $N-1$ neutral formamide molecules linked by single N–H...O=C hydrogen bonds. We can have a pictorial view of the solvated anion formation if we consider the most stable configurations of the neutral parents as hairpins made from two anti-parallel chains of dipoles which are zipped by hydrogen bonds. When an excess electron is added, these hairpins unzip by breaking bonds between the two chains which transform into a single chain of $N-1$ dipoles surrounding the negatively-charged monomer anion.

From the energies of the optimised neutral and the different anion structures for $N = 2$ to 7 calculated at the B3LYP 6-31G* level, we obtain the solvation energies $E_{sol}^{neutral}(N)$ and $E_{sol}^{anion}(N)$ that are plotted as a function of N in Figure 5.

Using inequality (2), we obtain a bracketing of the adiabatic electron affinity of isolated formamide -1.88 eV $\leq AEA(F) \leq -1.70$ eV. This value is less negative than the experimental vertical affinity VEA(F) value of -2.05 eV, in qualitative agreement with expectation. For comparison, the predicted value of the AEA from G2 calculations [46] is -1.58 eV. Using a mean value of -1.79 eV of AEA(F) in equation (1), we obtain the variation of the adiabatic electron affinities of formamide clusters as a function of size which is displayed in Figure 6.

4 Conclusion

We here provide the experimental value of the vertical valence electron affinity of the isolated formamide molecule and the experimental value of the cluster size threshold for observation of valence anions. The quantum calculations which are presented allow us to extract from those experimental data information about the adiabatic valence electron affinity of the isolated formamide molecule. In fact, since this electron affinity is strongly negative, the valence formamide anion has such a short lifetime that it autodetaches before relaxing and thus the meaning of adiabatic valence electron affinity is most probably dubious. However, in the case of homogeneous clusters, the calculations show that electron attachment takes place nearly entirely on a single molecule. Above $N = 5$, this electron attaching molecule is situated at the positive extremity of the dipole chain and the long range dipole-field may play a role for this localization. Following this first step, the cluster anion rearranges. The negatively-charged monomer becomes solvated by the neutral dipole chain which remains nearly intact but hydrogen bonds are broken. These predictions might be supported by photoelectron spectroscopy. The here presented anion structures have been deduced from DFT calculations but only up to limited sizes ($N = 7$). Qualitatively, these structures can be explained through the formation of a chain of neutrals constituting a dipole chain and surrounding a negatively-charged molecule, emphasizing the role of electrostatic interactions. In reference [19], a spiral arrangement of amide molecules or a block structure with cyclic units were proposed to explain a propensity observed in anion distributions. From the present results, it seems that the latter structure is more likely.

References

1. E. Fermi, E. Teller, Phys. Rev. **72**, 399 (1947)
2. P. Skurski, J. Simons, J. Chem. Phys. **112**, 6562 (2000)
3. H. Haberland, H. Ludewigt, C. Schindler, D.R. Worsnop, Phys. Rev. A **36**, 967 (1987)
4. J. Kalcher, *Theoretical prospects of negative ions* (Research SignPost, Trivandrum, India, 2002)
5. J.R.R. Verlet, A.E. Bragg, A. Kammrath, O. Chesnowsky, D.M. Neumark, Science **307**, 93 (2005)

6. E. Illenberger, Chem. Rev. **92**, 1589 (1992)
7. H. Abdoul-Carime, J.P. Schermann, C. Desfrançois, Few-Body Systems **31**, 183 (2002)
8. H.M. Lee, S.B. Suh, K.S. Kim, J. Chem. Phys. **118**, 9981 (2003)
9. J.W. Shin, N.I. Hammer, J.M. Headrick, M.A. Johnson, Chem. Phys. Lett. **399**, 349 (2004)
10. H. Haberland, C. Schindler, H.G. Worsnop, Ber. Bunsenges. Phys. Chem. **88**, 270 (1984)
11. J.V. Coe, G.H. Lee, J.G. Eaton, S.T. Arnold, H.W. Sarkas, K.H. Bowen, C. Ludewigt, H. Haberland, D.R. Worsnop, J. Chem. Phys. **92**, 3980 (1990)
12. C. Desfrançois, A. Lisfi, J.P. Schermann, Z. Phys. D **24**, 297 (1992)
13. G.J. Schulz, Rev. Mod. Phys. **45**, 378 (1973)
14. L. Sanche, G.J. Schulz, Phys. Rev. A **5**, 1672 (1972)
15. K. Harth, M.-W. Rüf, H. Hotop, Z. Phys. D **14**, 149 (1989)
16. C. Desfrançois, V. Périquet, S. Carles, J.P. Schermann, L. Adamowicz, Chem. Phys. **239**, 475 (1998)
17. B. Lucas, F. Lecomte, B. Reimann, H.D. Barth, G. Grégoire, Y. Bouteiller, J.P. Schermann, C. Desfrançois, Phys. Chem. Chem. Phys. **6**, 2600 (2004)
18. C.C. Wu, J.C. Jiang, I. Hahndorf, C. Chaudhuri, Y.T. Lee, H.C. Chang, J. Phys. Chem. A **104**, 9556 (2000)
19. T. Maeyama, N. Mikami, Phys. Chem. Chem. Phys. **6**, 1137 (2003)
20. A. Modelli, D. Jones, G. Distefano, Chem. Phys. Lett. **86**, 434 (1982)
21. A.R. Johnston, P.D. Burrow, J. Electron. Spectrosc. Relat. Phenom. **25**, 119 (1982)
22. P.D. Burrow, J.A. Michejda, Chem. phys. Lett. **42**, 223 (1976)
23. A. Modelli, G. Distefano, D. Jones, Chem. Phys. **73**, 395 (1982)
24. A. Modelli, H.D. Martin, J. Phys. Chem. A **106**, 7271 (2002)
25. F.B. Dunning, J. Phys. B **28**, 1645 (1995)
26. M.J. Frisch, G.W. Trucks, H.B. Schlegel, H.B. Scuseria, G.E. Robb, M.A. Cheeseman, J.R. Zakrzewski, V.G. Montgomery, J.A. Stratmann, R.E. Burant, J.C. Dapprich, S. Millam, J.M. Daniels, A.D. Kudin, K.N. Strain, M.O. Farkas, O. Tomasi, J. Barone, V. Cossi, M. Cammi, R. Mennucci, B. Pomelli, C. Adamo, C. Clifford, S. Ochterski, J. Petersson, G.A. Ayala, Q.P.Y. Cui, K. Morokuma, K. Malick, D.K. Rabuck, A.D. Raghavachari, K. Foresman, J.B. Cioslowski, J. Ortiz, J.V. Stefanov, B.B. Liu, G. Liashenko, A. Piskorz, P. Komaromi, I. Gomperts, R. Martin, R.L. Fox, D.J. Keith, T. Al-Laham, M.A. Peng, C.Y. Nanayakkara, A. Gonzalez, C. Challacombe, M. Gill, P.M.W. Johnson, B. Chen, W. Wong, M.W. Andres, J.L. Head-Gordon, E.S. Replogle, J.A. Popple, Revision A6 ed. (Pittsburg, PA, 1998)
27. C. Desfrançois, Y. Bouteiller, J.P. Schermann, D. Radisic, S.T. Stockes, K.H. Bowen, N.I. Hammer, R.N. Compton, Phys. Rev. Lett. **92**, 083003 (2004)
28. A. Modelli, Trends Chem. Phys. **6**, 57 (1997)
29. D. Chen, G.A. Gallup, J. Chem. Phys. **93**, 8893 (1990)
30. S.S. Staley, J.T. Strnad, J. Phys. Chem. **98**, 161 (1994)
31. J.S. Chao, M.F. Falcetta, K.D. Jordan, J. Chem. Phys. **93**, 1125 (1990)
32. A. Modelli, Phys. Chem. Chem. Phys. **5**, 2923 (2003)
33. A. Modelli, B. Hajgato, J.F. Nixon, L. Nyulaszi, J. Phys. Chem. A **108**, 7440 (2004)
34. N. Heinrich, W. Koch, G. Frenking, Chem. Phys. Lett. **124**, 20 (1986)
35. A. Pelc, W. Sailer, P. Scheier, M. Probst, N.J. Mason, E. Illenberger, T.D. Märk, Chem. Phys. Lett. **361**, 277 (2002)
36. J.W. Shin, N.I. Hammer, M.A. Johnson, H. Schneider, A. Glob, J.M. Weber, J. Phys. Chem. A (2005)
37. V. Périquet, A. Moreau, S. Carles, J.P. Schermann, C. Desfrançois, J. Electr. Spectr. Rel. Phenom. **106**, 141 (2000)
38. K.T. No, O.Y. Kwon, S.Y. Kim, M.S. Jhon, H.A. Scheraga, J. Phys. Chem. **99**, 3478 (1995)
39. R. Ludwig, F. Weinhold, T.C. Farrar, J. Chem. Phys. **103**, 3636 (1995)
40. M.C. Bellissent-Funel, S. Nasr, L. Bosio, J. Chem. Phys. **106**, 7913 (1997)
41. C.N. Tam, P. Bour, J. Eckert, F.R. Trouw, J. Phys. Chem. A **101**, 5877 (1997)
42. K.P. Sagarik, R. Ahlrichs, J. Phys. Chem. **86**, 5117 (1987)
43. S. Suhai, J. Chem. Phys. **103**, 7030 (1995)
44. S. Suhai, J. Phys. Chem. **100**, 3950 (1996)
45. E. Cabaleiro-Lago, M.A. Rios, J. Chem. Phys. **110**, 6782 (1999)
46. J.B. Foresman, A. Frisch, *Exploring Chemistry with Electronic Structure methods* (Gauusian, Inc, Pittsburg, US, 1996)
47. C. Desfrançois, H. Abdoul-Carime, J.P. Schermann, Int. J. Mod. Phys. **10**, 1339 (1996)